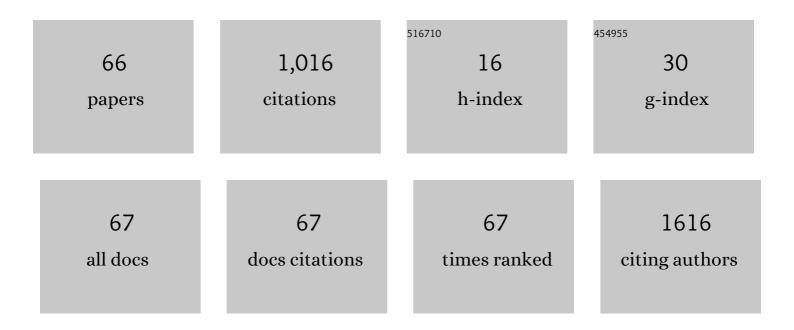
List of Publications by Year in descending order

Source: https://exaly.com/author-pdf/6873557/publications.pdf Version: 2024-02-01



#	ARTICLE	IF	CITATIONS
1	Reply to: Mild Chronic Colitis Triggers Parkinsonism in LRRK2 Mutant Mice through Activating TNFâ€Î± Pathway. Movement Disorders, 2022, 37, 665-666.	3.9	0
2	Mild Chronic Colitis Triggers Parkinsonism in <scp><i>LRRK2</i></scp> Mutant Mice Through Activating <scp>TNF</scp> â€i± Pathway. Movement Disorders, 2022, 37, 745-757.	3.9	23
3	Diabetic visceral neuropathy of gastroparesis: Gastric mucosal innervation and clinical significance. European Journal of Neurology, 2022, 29, 2097-2108.	3.3	4
4	Neuroinflammation in Low-Level PM2.5-Exposed Rats Illustrated by PET via an Improved Automated Produced [¹⁸ F]FEPPA: A Feasibility Study. Molecular Imaging, 2022, 2022, .	1.4	1
5	Effects of Focal Radiation on [18F]-Fluoro-D-Glucose Positron Emission Tomography in the Brains of Miniature Pigs: Preliminary Findings on Local Metabolism. Neuromodulation, 2021, 24, 863-869.	0.8	7
6	Endoscopic ultrasound ablation in a patient with multiple metastatic pancreatic tumors from adrenocorticotropic hormoneâ€producing thymic neuroendocrine neoplasm. Digestive Endoscopy, 2021, 33, 458-463.	2.3	2
7	<scp>PET</scp> / <scp>MRI</scp> in Cervical Cancer: Associations Between Imaging Biomarkers and Tumor Stage, Disease Progression, and Overall Survival. Journal of Magnetic Resonance Imaging, 2021, 53, 305-318.	3.4	9
8	A <scp>Doubleâ€Blind</scp> , Randomized, Controlled Trial of Lovastatin in <scp>Earlyâ€Stage</scp> Parkinson's Disease. Movement Disorders, 2021, 36, 1229-1237.	3.9	22
9	Preoperative 2-[18F]FDG PET-CT aids in the prognostic stratification for patients with primary ampullary carcinoma. European Radiology, 2021, 31, 8040-8049.	4.5	4
10	Metabolic Alterations in Pancreatic Cancer Detected by In Vivo 1H-MR Spectroscopy: Correlation with Normal Pancreas, PET Metabolic Activity, Clinical Stages, and Survival Outcome. Diagnostics, 2021, 11, 1541.	2.6	5
11	Long-term prognostic value of computed tomography-based attenuation correction on thallium-201 myocardial perfusion imaging: A cohort study. PLoS ONE, 2021, 16, e0258983.	2.5	5
12	2021 Advocacy Statements for the Role of Tc-Pyrophosphate Scintigraphy in the Diagnosis of Transthyretin Cardiac Amyloidosis: A Report of the Taiwan Society of Cardiology and the Society of Nuclear Medicine of the Republic of China. Acta Cardiologica Sinica, 2021, 37, 221-231.	0.2	2
13	Synthesis and analysis of 4-(3-fluoropropyl)-glutamic acid stereoisomers to determine the stereochemical purity of (4S)-4-(3-[18F]fluoropropyl)-L-glutamic acid ([18F]FSPG) for clinical use. PLoS ONE, 2020, 15, e0243831.	2.5	5
14	Title is missing!. , 2020, 15, e0243831.		0
15	Title is missing!. , 2020, 15, e0243831.		0
16	Title is missing!. , 2020, 15, e0243831.		0
17	Title is missing!. , 2020, 15, e0243831.		0

#	Article	IF	CITATIONS
19	Title is missing!. , 2020, 15, e0243831.		Ο
20	A Higher Preoperative Glycemic Profile Is Associated with Rapid Gastric Emptying After Sleeve Gastrectomy for Obese Subjects. Obesity Surgery, 2019, 29, 569-578.	2.1	10
21	Prospective comparison of (4S)-4-(3-18F-fluoropropyl)-l-glutamate versus 18F-fluorodeoxyglucose PET/CT for detecting metastases from pancreatic ductal adenocarcinoma: a proof-of-concept study. European Journal of Nuclear Medicine and Molecular Imaging, 2019, 46, 810-820.	6.4	15
22	Improved diagnostic accuracy of thallium-201 myocardial perfusion single-photon emission computed tomography with CT attenuation correction. Journal of Nuclear Cardiology, 2019, 26, 1584-1595.	2.1	13
23	Multiparametric PET/MR imaging biomarkers are associated with overall survival in patients with pancreatic cancer. European Journal of Nuclear Medicine and Molecular Imaging, 2018, 45, 1205-1217.	6.4	35
24	Clinical Utility of FDG PET/CT in Patients with Autoimmune Pancreatitis: a Case-Control Study. Scientific Reports, 2018, 8, 3651.	3.3	38
25	Diagnostic and Prognostic Implications of Exercise Treadmill and Rest First-Pass Radionuclide Angiography in Patients With Pulmonary Hypertension. Clinical Nuclear Medicine, 2017, 42, e392-e399.	1.3	3
26	Longitudinal evaluation of myocardial glucose metabolism and contractile function in obese type 2 diabetic db/db mice using small-animal dynamic 18F-FDG PET and echocardiography. Oncotarget, 2017, 8, 87795-87808.	1.8	11
27	Clinical significance of right ventricular activity on treadmill thallium-201 myocardial single-photon emission computerized tomography using cadmium–zinc–telluride cameras. Nuclear Medicine Communications, 2016, 37, 650-657.	1.1	8
28	A High Circulating Tumor Cell Count in Portal Vein Predicts Liver Metastasis From Periampullary or Pancreatic Cancer. Medicine (United States), 2016, 95, e3407.	1.0	80
29	Search of Unknown Fever Focus Using PET in Critically Ill Children With Complicated Underlying Diseases. Pediatric Critical Care Medicine, 2016, 17, e58-e65.	0.5	14
30	PET/MRI in pancreatic and periampullary cancer: correlating diffusion-weighted imaging, MR spectroscopy and glucose metabolic activity with clinical stage and prognosis. European Journal of Nuclear Medicine and Molecular Imaging, 2016, 43, 1753-1764.	6.4	59
31	Pregnancy Outcome After I-131 Therapy for Patients With Thyroid Cancer. Medicine (United States), 2016, 95, e2685.	1.0	19
32	Diagnostic Performance of Attenuation-Corrected Myocardial Perfusion Imaging for Coronary Artery Disease: A Systematic Review and Meta-Analysis. Journal of Nuclear Medicine, 2016, 57, 1893-1898.	5.0	51
33	18F-NaF PET/CT Images of Cardiac Metastasis From Osteosarcoma. Clinical Nuclear Medicine, 2016, 41, 708-709.	1.3	17
34	Comparison of biventricular ejection fractions using cadmium-zinc-telluride SPECT and planar equilibrium radionuclide angiography. Journal of Nuclear Cardiology, 2016, 23, 348-361.	2.1	16
35	The Incremental Diagnostic Performance of Coronary Computed Tomography Angiography Added to Myocardial Perfusion Imaging in Patients with Intermediate-to-High Cardiovascular Risk. Acta Cardiologica Sinica, 2016, 32, 145-55.	0.2	11
36	Patterns of Nodal Metastases on 18F-FDG PET/CT in Patients With Esophageal Squamous Cell Carcinoma are Useful to Guide Treatment Planning of Radiotherapy. Clinical Nuclear Medicine, 2015, 40, 384-389.	1.3	7

#	Article	IF	CITATIONS
37	Data-driven respiratory motion tracking and compensation in CZT cameras: A comprehensive analysis of phantom and human images. Journal of Nuclear Cardiology, 2015, 22, 308-318.	2.1	34
38	Incremental Diagnostic Performance of Combined Parameters in the Detection of Severe Coronary Artery Disease Using Exercise Gated Myocardial Perfusion Imaging. PLoS ONE, 2015, 10, e0134485.	2.5	9
39	Normal values and symptom correlation of a simplified oatmealâ€based gastric emptying study in the <scp>C</scp> hinese population. Journal of Gastroenterology and Hepatology (Australia), 2014, 29, 1873-1882.	2.8	13
40	Prognostic value of semiquantification NP-59 SPECT/CT in primary aldosteronism patients after adrenalectomy. European Journal of Nuclear Medicine and Molecular Imaging, 2014, 41, 1375-1384.	6.4	22
41	Preoperative Diagnosis of Pyoadenomyosis With 67Ga SPECT/CT. Clinical Nuclear Medicine, 2014, 39, e274-e276.	1.3	4
42	Corrigendum to "Atypical Thymic Carcinoid Associated with Coronary Artery Spasm: Incidental Finding of Myocardial Perfusion Imaging―[Int J Cardiol 161/2 (2012) e31–e33]. International Journal of Cardiology, 2013, 169, 154.	1.7	0
43	Left ventricle metastasis of esophageal cancer mimicking myocardial infarction in myocardial perfusion scintigraphy. International Journal of Cardiology, 2013, 167, e184-e186.	1.7	8
44	Usefulness of PET/CT for the Differentiation and Characterization of Periampullary Lesions. Clinical Nuclear Medicine, 2013, 38, 703-708.	1.3	12
45	67Ga SPECT/CT Aids in the Diagnosis of Occult Infected Common Iliac Artery Aneurysm. Clinical Nuclear Medicine, 2013, 38, 573-575.	1.3	4
46	Asymmetric Intense Bilateral Adrenal Uptake on [18F]Fluorodeoxyglucose Positron Emission Tomography/Computed Tomography in a Patient With Solitary Pulmonary Nodule. Journal of Clinical Oncology, 2012, 30, e83-e85.	1.6	3
47	Postoperative Lymphocele Demonstrated by Lymphoscintigraphy SPECT/CT. Clinical Nuclear Medicine, 2012, 37, 374-376.	1.3	6
48	Atypical thymic carcinoid associated with coronary artery spasm: Incidental finding of myocardial perfusion imaging. International Journal of Cardiology, 2012, 161, e31-e33.	1.7	2
49	Comparative study between endoscopic ultrasonography and positron emission tomography-computed tomography in staging patients with esophageal squamous cell carcinoma. Ecological Management and Restoration, 2012, 25, 40-47.	0.4	33
50	Sex-specific normal limits of left ventricular ejection fraction and volumes estimated by gated myocardial perfusion imaging in adult patients in Taiwan. Nuclear Medicine Communications, 2011, 32, 113-120.	1.1	15
51	Diagnostic value of 18F-FDC-PET/CT in indeterminate infiltrative hepatic lesions in an endemic area of viral hepatitis. Nuclear Medicine Communications, 2011, 32, 252-259.	1.1	3
52	Gallium-67 SPECT/CT for Abdominal Abscess. Clinical Nuclear Medicine, 2011, 36, 258-260.	1.3	6
53	The Role of Lymphoscintigraphy in Diagnosis and Monitor the Response of Physiotherapeutic Technique in Congenital Lymphedema. Clinical Nuclear Medicine, 2011, 36, e11-e12.	1.3	11
54	Cerebral Perfusion Changes in Hemiplegic Migraine. Clinical Nuclear Medicine, 2010, 35, 456-458.	1.3	12

#	Article	IF	CITATIONS
55	Correlation of F-18 fluorodeoxyglucose-positron emission tomography maximal standardized uptake value and EGFR mutations in advanced lung adenocarcinoma. Medical Oncology, 2010, 27, 9-15.	2.5	61
56	The diagnostic and prognostic effectiveness of F-18 sodium fluoride PET-CT in detecting bone metastases for hepatocellular carcinoma patients. Nuclear Medicine Communications, 2010, 31, 637-645.	1.1	55
57	¹³¹ I-6β-Iodomethyl-19-Norcholesterol SPECT/CT for Primary Aldosteronism Patients with Inconclusive Adrenal Venous Sampling and CT Results. Journal of Nuclear Medicine, 2009, 50, 1631-1637.	5.0	103
58	Usefulness of ²⁰¹ TL SPECT/CT relative to ¹⁸ Fâ€FDG PET/CT in detecting recurrent skull base nasopharyngeal carcinoma. Head and Neck, 2009, 31, 717-724.	2.0	8
59	Myocardial Infarction Without Coronary Artery Stenosis Illustrated by Tc-99m Pyrophosphate Scan, Cardiac Magnetic Resonance Imaging, and Myocardial Perfusion Scintigraphy. Clinical Nuclear Medicine, 2009, 34, 734-736.	1.3	0
60	Abnormal Myocardial Perfusion Imaging After Percutaneous Coronary Intervention Without Obstructing Lesion. Clinical Nuclear Medicine, 2009, 34, 38-39.	1.3	0
61	Unusual Finding of Thoracic Kidney on Myocardial Perfusion Imaging Using SPECT/CT. Clinical Nuclear Medicine, 2009, 34, 379-380.	1.3	3
62	18F-FDG PET for the lymph node staging of non-small cell lung cancer in a tuberculosis-endemic country: Is dual time point imaging worth the effort?. European Journal of Nuclear Medicine and Molecular Imaging, 2008, 35, 1305-1315.	6.4	68
63	Usefulness of Lymphoscintigraphy in Demonstrating Lymphedema in Patients With Noonan Syndrome. Clinical Nuclear Medicine, 2008, 33, 226-227.	1.3	4
64	F-18 Fluorodeoxyglucose Uptake in Gastric Adenoma After Stomach Distention by Water. Clinical Nuclear Medicine, 2008, 33, 643-644.	1.3	0
65	F-18 FDG PET/CT Illustrating Tumor Invasion in the IVC From Adrenocortical Carcinoma. Clinical Nuclear Medicine, 2007, 32, 891-892.	1.3	5
66	Extensive scar myocardium in hypertrophic cardiomyopathy with severe myocardial bridge. International Journal of Cardiology, 2007, 115, e105-e107.	1.7	7